ACTA ONCOLOGICA
2022, VOL. 61, NO. 6, 698–704
https://doi.org/10.1080/0284186X.2022.2062682

Taylor & Francis
Taylor & Francis Group

ORIGINAL ARTICLE



# Radiation-induced prostate swelling during SBRT of the prostate

Antti Vanhanen[a,b], Petri Reinikainen[a] and Mika Kapanen[b]

[a]Department of Oncology, Unit of Radiotherapy, Tampere University Hospital, Tampere, Finland; [b]Department of Medical Physics, Medical Imaging Center, Tampere University Hospital, Tampere, Finland

**ABSTRACT**

**Background:** Reduced planning target volume (PTV) margins are commonly used in stereotactic body radiotherapy (SBRT) of the prostate. In addition, MR-only treatment planning is becoming more common in prostate radiotherapy and compared to CT-MRI-based contouring results in notable smaller clinical target volume (CTV). Tight PTV margins coupled with MR-only planning raise a concern whether the margins are adequate enough to cover possible volumetric changes of the prostate. The aim of this study was to evaluate the volumetric change of the prostate and its effect on PTV margin during 5x7.25 Gy SBRT of the prostate.

**Material and Methods:** Twenty patients were included in the study. Three MRI scans, first prior to treatment (baseline), second after third fraction (mid-treatment) and third after fifth fraction (end-treatment) were acquired for each patient. Prostate contours were delineated on each MRI scan and used to assess the prostate volume and maximum prostate diameter on left-right (LR), anterior-posterior (AP) and superior-inferior (SI) directions at baseline, mid- and end-treatment.

**Results:** Median (IQR) change in the prostate volume relative to the baseline was 12.0% (3.1, 17.7) and 9.2% (2.0, 18.9) at the mid- and end-treatment, respectively, and the change was statistically significant ($p = 0.004$ and $p = 0.020$, respectively). Compared to the baseline, median increase in the maximum LR, SI and AP prostate diameters were 0.8, 2.3 and 1.5 mm at mid-treatment, and 0.5, 2.5 and 2.3 mm at end-treatment, respectively.

**Conclusion:** If prostate contouring is based solely on MRI (e.g., in MR-only protocol), additional margin of 1–2 mm should be considered to account for prostate swelling. The study is part of clinical trial NCT02319239.

**ARTICLE HISTORY**
Received 3 February 2022
Accepted 2 April 2022

**KEYWORDS**
SBRT of the prostate; MR-only; prostate swelling; PTV margin

## Background

Recent clinical studies have proven the feasibility of stereotactic body radiotherapy (SBRT) in the treatment of localized prostate cancer and it can be considered as an appropriate treatment modality for low-risk and intermediate-risk prostate cancer [1–4]. SBRT for high-risk prostate cancer is still recommended only under controlled trials due to lack of clinical evidence [5], but the overall number of SBRT treatments is expected to increase rapidly.

High fraction doses of SBRT and close proximity to critical organs such as rectum and bladder require increased precision in treatment planning and treatment execution. Therefore, modern treatment techniques with steep dose gradients and reduced treatment margins of 3 to 5 mm are recommended and commonly used in prostate SBRT [3,6].

Magnetic resonance (MR) imaging provides better soft tissue contrast than computed tomography (CT) enabling more accurate definition of the prostate [7,8] and is generally a prerequisite for prostate SBRT planning. Standard way is to use both MR and CT: MR for the target and organ at risk (OAR) delineation and the CT image for the dose calculation as it provides the required electron density information. CT and MR images are registered usually using intra-prostatic gold fiducial markers (FM). However, the CT-MR registration includes uncertainties and is associated with an error on the order of 2 mm [9,10]. This error should be taken into account when applying planning target volume (PTV) margins for clinical target volume (CTV). Often the anatomy differs between CT and MR images due to separate scanning instances and MR-based prostate definition may have to be adjusted to include prostate borders seen in CT image [11,12]. These limitations could be avoided by implementing MR-only treatment planning where CT scan is replaced with synthetic CT (S-CT) constructed from MR images scanned at the same imaging session as the planning MR images. MR-only planning has been introduced already for many years ago [13] and along with technological advancements it has gained special interest during the last decade [14–16]. MR-only based radiotherapy for prostate cancer has been clinically implemented [17–20] and owing to the emergence of commercial solutions for S-CT generation [21–24], it can be anticipated that the use of MR-only planning will increase.

Increased accuracy of MR-only protocol encourages to adapt the technique also for prostate SBRT. However, accurately delineated target volume coupled with reduced PTV

CONTACT Antti Vanhanen antti.vanhanen@pshp.fi Department of Oncology, Unit of Radiotherapy, Tampere University Hospital, Tampere, Finland
Supplemental data for this article can be accessed online at https://doi.org/10.1080/0284186X.2022.2062682.

margins raises a question of adequacy of the margins as the current knowledge on treatment efficiency is resulting from treatments executed with CT-based or CT-MR-based planning. Prostate volume is significantly smaller when delineation is based on MRI or combined use of MRI and CT instead of CT only: the reported ratio of the prostate volume between CT and MRI is 1.2–1.5 and the differences in prostate contours can be up to 6–8 mm at the apex and base of the prostate and smaller elsewhere [7,11,25,26]. When applying tight PTV margins around MR-only derived prostate, changes in prostate shape and size or prostate intrafraction motion, or the combination of both, may compromise target dose coverage at the treatment.

King *et al.* [27] utilized intraprostatic transponders to calculate prostate volumes at various time points throughout a conventionally fractionated treatment course and found that the prostate volume increases for most patients during the initial phase of the course after which it decreases significantly by the last day of the treatment. Maximum increase averaging 6.1% occurred at a median of seven days into the treatment [27]. Gunnlaugsson et al. [28] observed significant prostate swelling during and after an extremely hypofractionated treatment and came to a conclusion that the swelling would require up to 2 mm extra margin if prostate was defined solely on MRI. The patients of the study were treated according to HYPO-RT-PC study protocol with $7 \times 6.1$ Gy fractions, large 7 mm PTV margins and CTV delineation based on CT [28]. The purpose of the current study was to examine prostate volume changes and evaluate their effect on PTV margins when using more common $5 \times 7.25$ Gy fractionation and modern treatment technique with tighter 5 mm PTV margins – and confirm the results of Gunnlaugsson et al. [28] at the same time.

## Material and methods

### Patients and treatment planning

Twenty prostate patients treated between April 2016 and October 2017 were included in the study, which was part of a clinical trial (ClinicalTrials.gov NCT02319239). Inclusion criteria for the trial were: men up to 85 years of age with a biopsy-proven localized T1c-T2cN0M0 prostate carcinoma with one or two of the following intermediate risk factors: T2b-T2c, Gleason score 7 or prostate specific antigen (PSA) 10–20 ng/mL. Prostate cancer–specific exclusion criteria were the need for androgen deprivation therapy (ADT) or transurethral resection of the prostate (TURP). Other exclusion criteria included hip prosthesis, previous pelvic RT and another active malignancy in the previous five years. Median (range) age of the patients in this study was 70 (63–75) years with mean (range) psa of 9.98 (4.3–19.1) ng/mL. Four patients had Gleason score $3+3$, fifteen $3+4$ and one $4+3$.

Patients were treated according to our clinical protocol for prostate SBRT, with $5 \times 7.25$ Gy fractionation using two-arc volumetric modulated arc therapy (VMAT) technique and 10 MV flattening filter free (FFF) beams. Treatments were carried out with Varian TrueBeam STx linac (Varian Medical Systems, Palo Alto, CA). Three gold seed fiducial markers (FM) (Gold lock 3, Beam Point AB, Sweden) were implanted into the prostate median 8 days prior to planning MRI and CT. CTV was prostate and the proximal 5 mm of seminal vesicles (SV). The delineation was based on both the planning MRI and the CT images, both having 2 mm slice thickness. The PTV was formed adding 5 mm isotropic margin around the CTV. Target and risk organ delineation as well as dose optimization and calculation were made with Eclipse treatment planning system (TPS) (Varian Medical Systems, Palo Alto, CA), version 13.6. Dose was normalized so that the PTV mean dose was 100% of prescribed dose. Dose to the 95% volume of the PTV had to be at least 95% of the prescribed dose and maximum allowed PTV dose was 105% of the prescribed dose. Simultaneously, urethra region was spared by optimizing 7 Gy per fraction to urethra planning risk volume (PRV). Urethra PRV was formed by drawing 8 mm diameter circular margin around the center point of the urethra on each axial MRI slice. Treatment localization consisted of CBCT for checking of bladder and rectum filling status after which the position was confirmed and if necessary adjusted for intrafraction prostate motion with FM based orthogonal kV imaging. Additional kV-image pair was acquired between the treatment arcs for checking and adjusting of any intrafraction motion occurred during the first treatment arc.

### Prostate volume analysis

Changes in prostate volume during the treatment course were assessed by analyzing MRI images: in addition to the planning MRI (baseline), two additional MRI scans were acquired after the third (mid-treatment) and fifth (end-treatment) fractions. The MRI system used was 3 T Siemens Trio-Tim. Axial T2-weighted turbo spin echo (TSE) images (FOV $200 \times 200$ mm, resolution $0.625 \times 0.625$ mm, 2 mm slice thickness) were used for the prostate contouring and the contouring was done by the same radiation oncologist for all patients and images. The delineation was carried out in Eclipse TPS (Varian Medical Systems, Palo Alto, CA) as for the treatment planning. For prostate volume analysis, the prostate was contoured as prostate gland only, without the SVs and the contouring was done similarly for baseline, mid-treatment and end-treatment MRI scans each, totaling 60 different prostate structures. To reduce possible variation in contouring over time, the contouring was carried out in two working periods, dedicated solely for this purpose. Volume and maximum diameter of the prostate in anterior-posterior (AP), superior-inferior (SI) and left-right (LR) directions were recorded from the contoured images. The volume and maximum diameters from mid- and end-treatment MRI images were compared to the values obtained from the baseline MRI images. To check possible bias in contouring, 10 randomly selected MRI images were re-contoured by the same radiation oncologist in a subsequent session and the obtained volumes were compared to previously assessed values. Wilcoxon signed rank test was used to test the significance of the differences in prostate volume and maximum diameter relative to the baseline. Kruskal–Wallis test was

used to test whether the swelling of the prostate was anisotropic. Normality of the volume and maximum diameter distributions was tested with Shapiro–Wilk test. Significance level in all tests was $p < 0.05$.

## Results

Mean (±SD) prostate volumes were 37.6 ± 11.7, 41.9 ± 14.1 and 40.7 ± 13.3 $cm^3$ at baseline, mid-treatment and end-treatment, respectively (Figure 1). Median (interquartile range (IQR) in brackets) change in prostate volume relative to the baseline was 12.0% (3.1, 17.7) and 9.2% (2.0, 18.9) at the mid- and end-treatment, respectively. Mean (±SD) change in the volume was 11 ± 13% and 8 ± 13% at the mid- and end-treatment, respectively. The change in prostate volume was statistically significant at the mid- ($p = 0.004$) and end-treatment ($p = 0.020$). Prostate volumes at baseline, mid-treatment and end-treatment for each individual patient are shown in Table 1. Compared to the baseline, prostate volume was larger for 16 and 15 patients after the third and fifth fractions, respectively (Figure 2). Figure 3 presents relative prostate volume at mid- and end-treatment as a function of baseline prostate volume. Correlation between initial prostate volume and changes in prostate volume was not found. Prostate volumes assessed from 10 randomly selected and re-contoured MRI images correlated well with the initially determined values (coefficient of determination $R^2 = 0.987$) (Supplementary Figure S1). Mean difference between re-contoured and initially determined volumes was −0.7 $cm^3$ (−1.2%), which correspond to −0.2 mm mean change (range −1.4 mm, 1.0 mm) in prostate diameter, if prostate was assumed as a sphere.

Compared to the baseline, median increase in the maximum LR, SI and AP prostate diameters were 0.8 (−0.3, 2.0) ($p = 0.135$), 2.3 (0.9, 4.0) ($p = 0.025$) and 1.5 (0.0, 3.5) mm ($p = 0.009$) at mid-treatment, and 0.5 (−1.6, 1.5) ($p = 0.686$), 2.5 (0.0, 4.0) ($p = 0.038$) and 2.3 (0.4, 2.7) mm ($p = 0.010$) at end-treatment, respectively (IQR in brackets) (Figure 4). Mean (±95% CI) increase in the maximum LR, SI and AP diameters were 0.7 ± 0.9, 1.7 ± 1.4 and 1.7 ± 1.1 mm at mid-treatment

**Table 1.** Prostate volumes assessed from MRI images prior to treatment (baseline) and after the third (mid-treatment) and fifth (end-treatment) fractions for each patient.

| Patient | Baseline Volume [$cm^3$] | Mid-treatment Volume [$cm^3$] | Mid-treatment Relative volume | End-treatment Volume [$cm^3$] | End-treatment Relative volume |
|---|---|---|---|---|---|
| 1 | 34.0 | 37.9 | 1.11 | 35.0 | 1.03 |
| 2 | 43.8 | 43.0 | 0.98 | 45.0 | 1.03 |
| 3 | 32.1 | 38.0 | 1.18 | 34.0 | 1.06 |
| 4 | 45.9 | 61.4 | 1.34 | 55.8 | 1.22 |
| 5 | 32.3 | 37.5 | 1.16 | 40.2 | 1.24 |
| 6 | 33.0 | 32.8 | 0.99 | 30.9 | 0.94 |
| 7 | 33.6 | 36.8 | 1.10 | 35.2 | 1.05 |
| 8 | 36.4 | 37.7 | 1.04 | 43.2 | 1.19 |
| 9 | 43.3 | 50.3 | 1.16 | 51.7 | 1.19 |
| 10 | 28.8 | 32.9 | 1.14 | 32.4 | 1.13 |
| 11 | 34.0 | 27.0 | 0.79 | 26.1 | 0.77 |
| 12 | 28.3 | 29.9 | 1.06 | 28.2 | 1.00 |
| 13 | 31.5 | 32.0 | 1.02 | 29.3 | 0.93 |
| 14 | 32.3 | 35.7 | 1.11 | 34.0 | 1.05 |
| 15 | 53.3 | 68.9 | 1.29 | 61.8 | 1.16 |
| 16 | 20.6 | 23.2 | 1.13 | 24.1 | 1.17 |
| 17 | 65.9 | 62.2 | 0.94 | 59.2 | 0.90 |
| 18 | 32.9 | 40.7 | 1.24 | 40.9 | 1.24 |
| 19 | 63.1 | 74.1 | 1.17 | 73.6 | 1.17 |
| 20 | 27.3 | 36.3 | 1.33 | 33.8 | 1.24 |
| Mean | 37.6 | 41.9 | 1.11 | 40.7 | 1.08 |
| SD | 11.7 | 14.1 | 0.13 | 13.3 | 0.13 |
| Median | 33.3 | 37.6 | 1.12 | 35.1 | 1.09 |

Mid- and end-treatment volumes relative to the baseline are also presented.

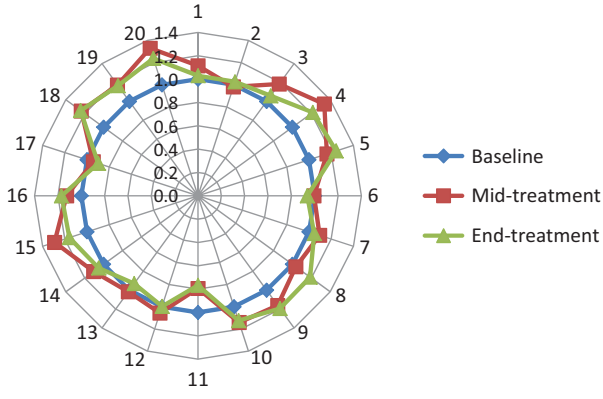


**Figure 2.** Change in prostate volume relative to baseline (=1) for each patient ($n = 20$).

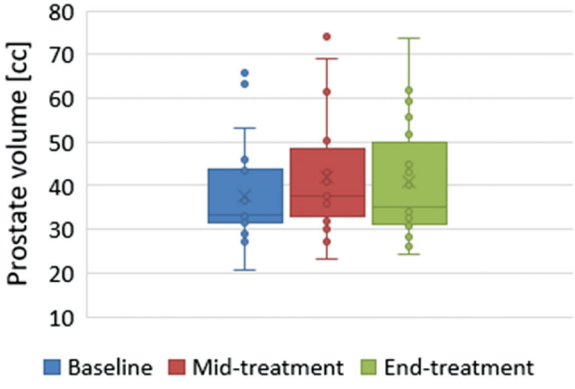


**Figure 1.** Prostate volume at baseline, mid- and end-treatments. The box limits represent the median and 25th and 75th percentiles and the cross shows the mean value. The whiskers extend up to the largest values that are less than or equal to 1.5 times the interquartile range or down to the smallest values that are larger than 1.5 times the interquartile range. Dots outside the whiskers represent outliers.

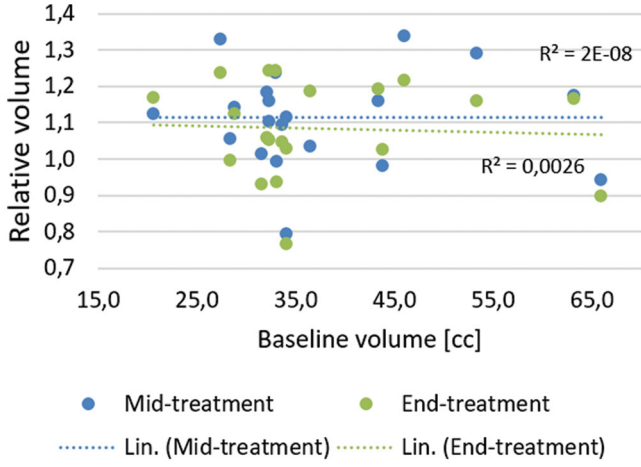


**Figure 3.** Prostate volume at the mid- and end-treatment relative to the baseline, as a function of baseline prostate volume.

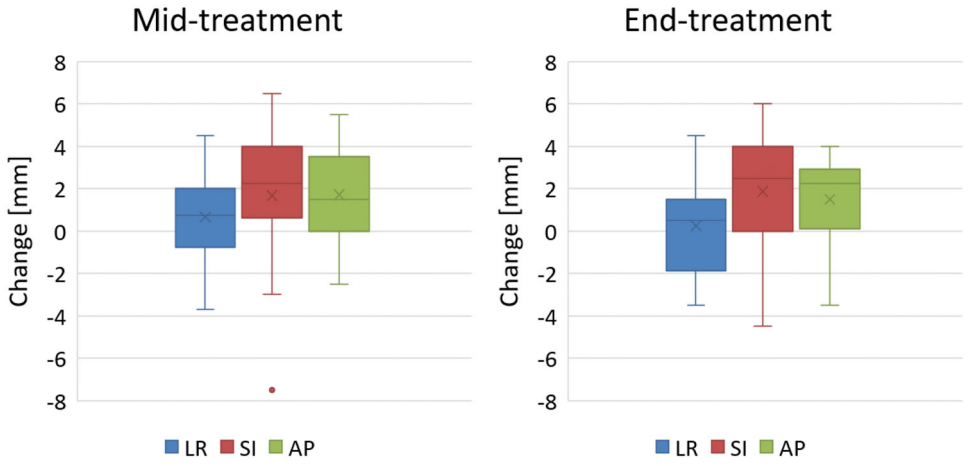


**Figure 4.** Change in maximum prostate diameter at mid- and end-treatment, relative to the baseline. The box limits represent the median and 25th and 75th percentiles and the cross shows the mean value. The whiskers extend up to the largest values that are less than or equal to 1.5 times the interquartile range or down to the smallest values that are larger than 1.5 times the interquartile range. Dots outside the whiskers represent outliers.

and $0.2 \pm 1.0$, $1.9 \pm 1.4$ and $1.5 \pm 0.9$ mm at end-treatment, respectively. All directions and mid- and end-treatment considered, in 90% (108/120) of the cases, swollen prostate would have been covered with 2 mm additional isotropic margin. Based on the Kruskal–Wallis test, there was not significant difference in prostate swelling (maximum diameter change) between different directions neither at the mid-treatment ($p = 0.158$), nor at the end-treatment ($p = 0.064$).

## Discussion

The results of this study indicate that the prostate volume increases during the $5 \times 7.25$ Gy ultrahypofractionated treatment and the increase is statistically significant. The increased volume at the mid-treatment seems to decrease toward the end of the treatment but is still larger than at the planning phase, prior to treatment. These results confirm the findings of Gunnlaugsson et al. [28] about the prostate volume increase during the $7 \times 6.1$ Gy ultrahypofractionated treatment. Compared to the baseline, they observed 14% mean increase at mid-treatment and 9% mean increase at end-treatment. The findings of this study are very similar, with 11% mean (12% median) and 8% mean (9% median) volume increase at mid- and end-treatment, respectively. In a recent article, Ma et al. studied prostate volume changes during MRI-guided ultrahypofractionated treatment with $5 \times 8$ Gy fractionation, and found median volume increase of 0.1, 9.0, 12.1, 15.1 and 14.2% at fractions 1–5, respectively [29]. As in our study (Figure 3), volume increase did not depend on baseline volume, which itself was significantly affected if hormonal treatment was used [29]. On the other hand, the use of ADT was associated with significantly smaller volume increase than without ADT [29]. Compared to our study, Ma et al. found larger prostate swelling at end-treatment. It can be pondered whether this is due to larger dose per fraction used in their study. Median prostate swelling of 9.1–9.5%, depending on the observer, between the first and subsequent fractions during $5 \times 7.25$ Gy prostate treatment has been reported also in another study using MRI-linac for the treatment [30].

Previous findings of prostate volume increase in conventionally fractionated prostate radiotherapy [27] indicate, that the radiation-induced prostate swelling is not only related to the high doses per fraction but the phenomenon seems to be greater with ultrahypofractionation. The swelling of the prostate seems to reach its maximum at the 3$^{rd}$–4$^{th}$ fraction of 5-fraction ultrahypofractionated treatment given every other day which correspond to the findings with conventional fractionation given every day [27–29]. The cause of the radiation-induced prostate swelling is not clear, but it may be associated with inflammation [29].

Based on the analysis of the maximum prostate diameters, the increase was largest at SI and AP directions and a bit smaller in LR direction. However, the differences between the directions were not statistically significant and agree with previous findings of isotropic increase in prostate volume [29]. Also the scale of the observed maximum diameter change was similar to previous findings, although Gunnlaugsson et al. observed no change in lateral maximum prostate diameter [28,29]. Gunnlaugsson et al. suggested that up to 2 mm margin extension could be needed to account for prostate swelling [28]. On the other hand, the dosimetric analysis of Ma et al. showed that despite the changes in prostate volume, 2 mm PTV margin was enough to secure at least 95% of the target volume to receive 95% of the prescription dose for 94% of the fractions. However, for proximal 1 cm of SVs, this criterion was fulfilled only for 59% of fractions [29]. SV interfractional motion and deformation larger than that of prostate are known phenomena and generally require larger margins than prostate gland [31–34]. SVs were not included in the prostate volume analysis in the current study. The analysis of Ma et al. ignores other factors affecting treatment margins and dose coverage such as prostate intrafraction motion or the accuracy of the technical equipment used for treatment localization and irradiation [29]. However, all of these factors add to the total geometric uncertainty of the treatment and should be considered carefully, when applying PTV margins in ultrahypofractionated prostate radiotherapy. This is especially important when converting from CT-MR-based planning to MR-only treatment planning, as the same margin would cover smaller volume in MR-only and

would not be as forgiving as for CT-MR-based planning. Margins required to account for intrafraction prostate motion depend greatly on localization method used and the duration of the treatment [35–37]. Intrafraction imaging or electromagnetic tracking and beam gating could be used to reduce the treatment margins and mitigate the effect of prostate motion. However, only recently introduced MR-linacs could provide exact information also from the prostate shape and size in treatment situation and if necessary, can be used for on-line adaptive radiotherapy [38,39]. The problem in daily adaptive planning is that it is still very time consuming and its benefit is counteracted by the volume changes in bladder and rectum and prostate intrafraction motion [40]. For now, MR-linacs are not widely available, but future development of the MRI-linacs and adaptive planning procedures could lead to wider implementation of the technique.

Additional margins needed to cover the prostate swelling can roughly be approximated by assuming prostate as a sphere. Its radius corresponding to a mean baseline volume observed in this study (37.6 $cm^3$) would be 2.08 cm. Increase of 10% and 15% in volume results in 2.15 cm and 2.18 cm radiuses, respectively. In other words, 1 mm extra margin would cover 15% prostate swelling in this ideal case. In this study, in 90% of the cases, prostate contours would have been covered with 2 mm additional isotropic margin, if the prostate swelling was assumed to be symmetrical about the main direction axes. As the magnitude of the swelling depends on the phase of the treatment course, the extra margin should be time dependent. Choosing a fixed margin could be suboptimal with regard to OAR exposure at the first 1–2 fractions. Altogether, when considering MR-only based treatment planning for ultrahypofractionated prostate radiotherapy, additional margin of 1-2 mm should be considered to account for prostate swelling.

As the larger margin size increases the dose to the nearby OARs, the margin should be kept as low as possible by accurate treatment localization, intrafraction imaging and shortening the treatment time by using modern treatment techniques such as VMAT and FFF beams. As the prostate intrafraction motion is non-Gaussian and its probability increases with time, optimal treatment margins would be non-isotropic, based on the observed motion pattern and duration of the treatment if intrafraction imaging-based beam gating is not an option [35,41,42].

Large variation was characteristic of both the measured change in prostate volume and maximum diameter, which could indicate the difficulty of defining prostate contours even from the MRI images. Prostate or patient motion during the imaging affects negatively the MR image quality and this was seen with two patients (patient number 17 and 18). For patient number 11, a notably smaller prostate volume than at the baseline was measured at the mid- and end-treatments. The patient had almost empty bladder at the baseline MR, whereas it was extremely full at the mid- and end-treatment MR scans. This could have caused pressure on the prostate resulting in a compressed volume. However, more detailed analysis of prostate deformation was out of scope of this study.

One of the limitations of the study was small sample size which was due to limited MRI resources. Another limitation was that the delineation was made by single oncologist, and therefore, we could not determine the effect of inter-observer variability on the observed prostate volume changes. On the other hand, this ensured that the measured prostate volumes for single patient were not affected by the inter-observer variation. Possible bias in contouring was checked by re-contouring ten randomly selected MRI images and comparing the obtained prostate volumes to initially determined values. Newly and initially assessed values correlated well, which suggests that the results obtained in this study are not biased. Small differences between the values can be explained by intraobserver variability, which can be as large as 3 mm at various points (e.g., prostate apex or base of the SVs) around the prostate [7]. Dosimetric effect of the volume changes were not assessed in this study, but as mentioned before, accurate simulation of the dosimetric effect would require motion-including dose reconstruction [43], which was out of scope of this study. Future investigation would include the determination of the combined effect of prostate volumetric changes and intrafraction prostate motion on prostate dose coverage.

## Conclusions

The findings of this study indicate that the prostate volume increases during the $5 \times 7.25$ Gy ultrahypofractionated radiotherapy treatment and the change in the volume is statistically significant. Swelling of the prostate was less pronounced in LR direction than in SI and AP directions but statistically significant differences between the directions were not found. Additional 1–2 mm margin to cover the prostate swelling should be considered, especially if the treatment planning is MR-only based. However, the uncertainty related to the prostate swelling should be taken into account when determining appropriate margins regardless of the planning method used.

## Disclosure statement

No potential conflict of interest was reported by the author(s).

## Funding

This study was supported by the Seppo Nieminen Fund of Tampere University Hospital Research Center under Grant 15012 and the Research funding provided by the Tampere University Hospital under Grant MJ0068.

## Funding

This study was supported by the Seppo Nieminen Fund of Tampere University Hospital Research Center under Grant 15012 and the Research funding provided by the Tampere University Hospital under Grant MJ0068.

## Data availability statement

Numerical data associated with the paper could be shared upon reasonable request from the corresponding author.

## References


[1] Widmark A, Gunnlaugsson A, Beckman K, et al. Ultra-hypofractionated versus conventionally fractionated radiotherapy for prostate cancer: 5-year outcomes of the HYPO-RT-PC randomized, non-inferiority, phase 3 trial. Lancet. 2019;394(10196):385–395.

[2] Kishan AU, Dang A, Katz AJ, et al. Long-term outcomes of stereotactic body radiotherapy for low-risk and intermediate-risk prostate cancer. JAMA Netw Open. 2019;2(2):e188006.

[3] Brand DH, Tree AC, Ostler P, PACE Trial Investigators, et al. Intensity-modulated fractionated radiotherapy versus stereotactic body radiotherapy for prostate cancer (PACE-B): acute toxicity findings from an international, randomised, open-label, phase 3, non-inferiority trial. Lancet Oncol. 2019;20(11):1531–1543.

[4] Jackson WC, Silva J, Hartman HE, et al. Stereotactic body radiation therapy for localized prostate cancer: a systematic review and Meta-analysis of over 6,000 patients treated on prospective studies. Int J Radiat Oncol Biol Phys. 2019;104(4):778–789.

[5] Foerster R, Zwahlen DR, Buchali A, et al. Stereotactic body radiotherapy for high-risk prostate cancer: a systematic review. Cancers. 2021;13(4):759.

[6] Loblaw A. Stereotactic ablative body radiotherapy for intermediate- or high-risk prostate cancer. Cancer J. 2020;26(1):38–42.

[7] Rasch C, Barillot I, Remeijer P, et al. Definition of the prostate in CT and MRI: a multi-observer study. Int J Radiat Oncol Biol Phys. 1999;43(1):57–66.

[8] Debois M, Oyen R, Maes F, et al. The contribution of magnetic resonance imaging to the three-dimensional treatment planning of localized prostate cancer. Int J Radiat Oncol Biol Phys. 1999; 45(4):857–865.

[9] Hamdan I, Bert J, Rest CCL, et al. Fully automatic deformable registration of pretreatment MRI/CT for image-guided prostate radiotherapy planning. Med Phys. 2017;44(12):6447–6455.

[10] Wegener D, Zips D, Thorwarth D, et al. Precision of T2 TSE MRI-CT-image fusions based on gold fiducials and repetitive T2 TSE MRI-MRI-fusions for adaptive IGRT of prostate cancer by using phantom and patient data. Acta Oncol. 2019;58(1):88–94.

[11] Gunnlaugsson A, Persson E, Gustafsson C, et al. Target definition in radiotherapy of prostate cancer using magnetic resonance imaging only workflow. Phys Imaging Radiat Oncol. 2019;9:89–91.

[12] Jonsson J, Nyholm T, Söderkvist K. The rationale for MR-only treatment planning for external radiotherapy. Clin Transl Radiat Oncol. 2019;18:60–65.

[13] Lee YK, Bollet M, Charles-Edwards G, et al. Radiotherapy treatment planning of prostate cancer using magnetic resonance imaging alone. Radiother Oncol. 2003;66(2):203–216.

[14] Devic S. MRI simulation for radiotherapy treatment planning. Med Phys. 2012;39(11):6701–6711.

[15] Kapanen M, Collan J, Beule A, et al. Commissioning of MRI-only based treatment planning procedure for external beam radiotherapy of prostate. Magn Reson Med. 2013;70(1):127–135.

[16] Paulson ES, Erickson B, Schultz C, et al. Comprehensive MRI simulation methodology using a dedicated MRI scanner in radiation oncology for external beam radiation treatment planning. Med Phys. 2015;42(1):28–39.

[17] Tenhunen M, Korhonen J, Kapanen M, et al. MRI-only based radiation therapy of prostate cancer: workflow and early clinical experience. Acta Oncol. 2018;57(7):902–907.

[18] Kerkmeijer LGW, Maspero M, Meijer GJ, et al. Magnetic resonance imaging only workflow for radiotherapy simulation and planning in prostate cancer. Clin Oncol (R Coll Radiol). 2018;30(11): 692–701.

[19] Tyagi N, Fontenla S, Zelefsky M, et al. Clinical workflow for MR-only simulation and planning in prostate. Radiat Oncol. 2017; 12(1):119.

[20] Christiansen RL, Jensen HR, Brink C. Magnetic resonance only workflow and validation of dose calculations for radiotherapy of prostate cancer. Acta Oncol. 2017;56(6):787–791.

[21] Köhler MVT, Grootel MV, Hoogeven R, et al. MR-only simulation for radiotherapy planning. Philips White Paper. 2015

[22] Tyagi N, Fontenla S, Zhang J, et al. Dosimetric and workflow evaluation of first commercial synthetic CT software for clinical use in pelvis. Phys Med Biol. 2017;62(8):2961–2975.

[23] Persson E, Gustafsson C, Nordström F, et al. MR-OPERA: a multicenter/multivendor validation of magnetic resonance imaging-only prostate treatment planning using synthetic computed tomography images. Int J Radiat Oncol Biol Phys. 2017; 99(3):692–700.

[24] MR-only RT planning for the brain and pelvis with synthetic CT. Siemens White paper. 2019.

[25] Hentschel B, Oehler W, Strauss D, et al. Definition of the CTV prostate in CT and MRI by using CT-MRI image fusion in IMRT planning for prostate cancer. Strahlenther Onkol. 2011;187(3): 183–190.

[26] Seppälä T, Visapää H, Collan J, et al. Converting from CT- to MRI-only-based target definition in radiotherapy of localized prostate cancer: A comparison between two modalities. Strahlenther Onkol. 2015;191(11):862–868.

[27] King BL, Butler WM, Merrick GS, et al. Electromagnetic transponders indicate prostate size increase followed by decrease during the course of external beam radiation therapy. Int J Radiat Oncol Biol Phys. 2011;79(5):1350–1357.

[28] Gunnlaugsson A, Kjellén E, Hagberg O, et al. Change in prostate volume during extreme hypo-fractionation analysed with MRI. Radiat Oncol. 2014;9:22.

[29] Ma TM, Neylon J, Casado M, et al. Dosimetric impact of interfraction prostate and seminal vesicle volume changes and rotation: a post-hoc analysis of a phase III randomized trial of MRI-guided versus CT-guided stereotactic body radiotherapy. Radiother Oncol. 2022;167:203–210.

[30] Willigenburg T, de Muinck Keizer DM, Peters M, et al. Evaluation of daily online contour adaptation by radiation therapists for prostate cancer treatment on an MRI-guided linear accelerator. Clin Transl Radiat Oncol. 2021;27:50–56.

[31] van der Wielen GJ, Mutanga TF, Incrocci L, et al. Deformation of prostate and seminal vesicles relative to intraprostatic fiducial markers. Int J Radiat Oncol Biol Phys. 2008;72(5):1604–1611.

[32] O'Neill AGM, Jain S, Hounsell AR, et al. Fiducial marker guided prostate radiotherapy: a review. Br J Radiol. 2016;89(1068): 20160296.

[33] Langen KM, Jones DT. Organ motion and its management. Int J Radiat Oncol Biol Phys. 2001;50(1):265–278.

[34] Mutanga TF, de Boer HC, van der Wielen GJ, et al. Margin evaluation in the presence of deformation, rotation, and translation in prostate and entire seminal vesicle irradiation with daily marker-based setup corrections. Int J Radiat Oncol Biol Phys. 2011;81(4): 1160–1167.

[35] Litzenberg DW, Balter JM, Hadley SW, et al. Influence of intrafraction motion on margins for prostate radiotherapy. Int J Radiat Oncol Biol Phys. 2006;65(2):548–553.

[36] Vanhanen A, Poulsen P, Kapanen M. Dosimetric effect of intrafraction motion and different localization strategies in prostate SBRT. Phys Med. 2020;75:58–68.

[37] Li JS, Lin MH, Buyyounouski MK, et al. Reduction of prostate intrafractional motion from shortening the treatment time. Phys Med Biol. 2013;58(14):4921–4932.

[38] Kim J, Park JM, Choi CH, et al. Retrospective study comparing MR-guided radiation therapy (MRgRT) setup strategies for prostate treatment: repositioning vs. replanning. Radiat Oncol. 2019; 14(1):139.

[39] Tetar SU, Bruynzeel AME, Lagerwaard FJ, et al. Clinical implementation of magnetic resonance imaging guided adaptive radiotherapy for localized prostate cancer. Phys Imaging Radiat Oncol. 2019;9:69–76.

[40] Mannerberg A, Persson E, Jonsson J, et al. Dosimetric effects of adaptive prostate cancer radiotherapy in an MR-linac workflow. Radiat Oncol. 2020;15(1):168.
[41] Lin Y, Liu T, Yang W, et al. The non-Gaussian nature of prostate motion based on real-time intrafraction tracking. Int J Radiat Oncol Biol Phys. 2013;87(2):363–369.
[42] Ballhausen H, Li M, Hegemann N-S, et al. Intra-fraction motion of the prostate is a random walk. Phys Med Biol. 2015;60(2):549–563.
[43] Poulsen PR, Schmidt ML, Keall P, et al. A method of dose reconstruction for moving targets compatible with dynamic treatments. Med Phys. 2012;39(10):6237–6246.